Mol Cell Biochem (2009) 330:83–95
DOI 10.1007/s11010-009-0103-8

Apoptosis induced by modulation in selenium status involves p38 MAPK and ROS: implications in spermatogenesis

Pavitra Ranawat · M. P. Bansal

Received: 3 February 2009 / Accepted: 30 March 2009 / Published online: 12 April 2009

Abstract Selenium has been linked to cell survival and apoptosis. Apoptosis plays an important role in spermatogenesis. Evidence suggests that reactive oxygen species induce apoptotic pathways. Although the mechanism by which oxidants mediate apoptosis is not well defined, the mitogen-activated protein kinase (MAPK) and caspase pathways have been implicated in apoptosis. Thus, this study was designed, keeping in view the critical balance between cell proliferation and apoptosis for normal spermatogenesis, and the requirement of selenium for the maintenance of male fertility. The intracellular selenium status was modulated by feeding selenium-deficient and -excess diet for 8 weeks. Involvement of p38 MAPK and ROS was monitored. Apoptotic factors like caspases and Bcl-2 were also analyzed. It was observed that the selenium levels were altered along with an increase in ROS generation and lipid peroxidation. mRNA expression of p38, caspases 3, and 8 increased, whereas that for Bcl-2 decreased. Western immunoblot analysis and immunohistochemical localization studies for p38 showed a similar increase. Integrity of DNA was altered in the form of apoptotic cells. Thus, the results presented in this study suggest that sodium selenite causes apoptosis and the toxicity of selenite is mediated by increase in ROS. Morevoer, ROS generation is associated with increased expression of p38, caspases 3 and 8, and decreased Bcl-2 expression. Our data indicate that p38 participates in testicular apoptosis and that selenium is required for maintenance of the critical balance between cell death and proliferation.

P. Ranawat · M. P. Bansal (✉)
Department of Biophysics, Panjab University,
Chandigarh 160014, India
e-mail: mpbansal@pu.ac.in

Keywords Selenium · Apoptosis · p38 MAPK · ROS · Caspase 3 · Csapase 8

Introduction

Selenium (Se), an essential trace element present in both prokaryotic and eukaryotic cells, has been linked to regulatory functions in cell growth, cell survival, cytotoxicity, and transformation [1]. Selenium appears to modulate such cellular activities presumably by acting on proteins important for signal transduction [2]. Nonetheless, the modulatory functions of selenite and other Se compounds on intracellular signaling pathways are not fully understood.

The reproductive organ appears to be a priority tissue for Se accumulation [3]. Selenium deficiency gives rise to testicular structural and functional disturbances and causes oxidative stress in the organ due to diminished antioxidant property of this element as a co-factor of GSH-Px [4]. At higher dose levels, Se causes many deleterious effects on various organs including testes.

Spermatogenesis, the complex process of male germ cell proliferation and maturation from diploid spermatogonia to mature haploid spermatozoa, takes place in the seminiferous epithelium of the testis. During this process, the number of germ cells has to match with the capacity of the somatic sertoli cells which provide the structural support and biochemical factors essential for germ cell development. In this regard, apoptotic cell death plays an important role in limiting the testicular germ cell population both in physiological conditions and under stress caused by external disturbances.

Studies have also demonstrated stimulation of apoptosis after Se supplementation at pharmacologic doses [5]. Moreover, low Se status can induce multiple transcriptional

pathways suggestive of oxidative stress, DNA damage, and alterations in cell-cycle progression, providing a framework for understanding the multiple roles of Se in human health [6].

Oxidative stress has been linked to apoptosis in various systems [7]. There is evidence that reactive oxygen species (ROS) play roles in the induction of both the death receptor and mitochondrial apoptotic pathways [8]. High ROS concentrations induce apoptotic cell death in various cell types [9], suggesting that ROS contribute to cell death whenever they are generated in the course of the apoptotic process. Endogenous production of ROS has also been associated with the induction of apoptosis [10]. However, there is controversy as to whether ROS signaling is critical for the induction of apoptosis or is merely a byproduct of apoptosis [9].

Although the mechanism by which oxidants mediate apoptosis is not well defined, the mitogen-activated protein kinase (MAPK) and caspase pathways have been implicated in apoptosis induced by a variety of apoptotic stimuli [11]. Stress stimuli activate MAPKs through phosphorylation. Several members of the MAPK family have been identified, including extracellular signal-regulated kinase (ERK) [12], c-Jun N-terminal protein kinase (SAPK/JNK) [13], and p38 MAP kinase [14]. Many subsequent studies have confirmed an anti-apoptotic role for ERK1/2 and a pro-apoptotic role for sustained activation of p38 and JNK [10].

The p38 kinase is an upstream kinase for transcription factor AP-1 which has been shown to be modulated by Se-induced stress by previous studies [15] in our lab. This modulation of AP-1 affects the reproductive potential and leads to decrease in sperm number, motility, and percentage fertility [15]. This stress-activated kinase p38, a serine/threonine kinase, is also activated in dying granulocytes [16]. Inhibition of p38 MAPK activity using synthetic inhibitors was reported to delay neutrophil apoptosis in culture [16].

In contrast to necrotic cell death, apoptosis is characterized by cell shrinkage, chromatin condensation, DNA fragmentation, and eventual disintegration into membrane-enclosed apoptotic bodies [17]. Caspases, a family of aspartate–cysteine proteases, are key effectors responsible for many morphological and biochemical changes in apoptosis [18]. Caspase-8 has been established as an important component of the FasR death-inducing signaling complex (DISC) [19]. Recently, the involvement of p38 in the activation of caspase-8 in dopaminergic neurons has been reported [20]. The effector caspase-3 also functions downstream of p38 [21].

Moreover, the cellular threshold for apoptosis is highly regulated by a growing number of Bcl-2 family of proteins [22]. Among the members, Bcl-2, a 25-kDa protein, and Bcl-x_L, a 30-kDa protein, are potent repressors of apoptosis. Studies have shown that overexpression of Bcl2 in germ cells inhibits the apoptotic wave followed by degeneration of germ cells in testes of transgenic adult mice [23].

Thus, keeping in view the critical balance between cell proliferation and apoptosis for normal spermatogenesis to take place, and the requirement of Se as an essential trace element for maintenance of male fertility, this study was designed. The intracellular Se status was modulated by respective diet feeding for 4 and 8 weeks, to study the role of Se in testicular cell sensitivity to apoptosis. Moreove, the involvement of p38 MAPK and ROS in the culmination of apoptosis was monitored with possible implications in spermatogenesis. The study was extended further to correlate with the corresponding apoptotic factors like caspases and Bcl-2.

Materials and methods

Chemicals

Sodium selenite (Na_2SeO_3), Dichlorofluorescin diacetate (DCFH-DA), 2,3-diaminonapthalene (DAN), Agarose, Ethidium bromide, and Proteinase K were purchased from Sigma-Aldrich (St. Louis, MO, USA). TRI-reagent and one-step RT-PCR kit were obtained from Molecular Research Centre (Inc. Cincinnati; Ohio) and QIAGEN, respectively. Oligonucleotides were synthesized by Sigma-Aldrich. Molecular biology grade chemicals for RNA isolation, e.g., chloroform, isopropanol, ethanol, and formaldehyde were purchased from Amresco, Ohio (USA).

Antibody against p38 was purchased from Santa Cruz Biotechnology, Santa Cruz, CA (USA); peroxidase-conjugated anti-rabbit secondary antibody and anti-mouse β-actin were purchased from Sigma-Aldrich, St Louis (USA). All other chemicals and reagents used in this study were of analytical grade and were procured from the Indian manufacturers.

Animal procurement and treatment schedule

Male Balb/c mice in the weight range of 20–25 g were used in this study. Animals were procured from the Central Animal House, Punjab University, Chandigarh (India). They were housed in a standard animal facility under controlled temperature and 12/12 h light/dark cycle with food and water provided ad libitum. This study was duly cleared with approval from the Institutional Animal Ethics Committee.

In order to make differential Se statuses in aminals viz., 0.02 ppm, 0.2 ppm, and 1 ppm, in different groups (Group I, II, and III, respectively), the mice were kept on

yeast-based diet. The yeast-based diet usually contains 0.02 ppm Se, and hence animals fed on this diet were considered Se-deficient animals (Group I). For Se-supplemented groups, Se was added at 0.2 ppm (Group II; adequate level) and 1 ppm (Group III; excess level) as sodium selenite to Se-deficient diet. All the animals were fed with the respective diets for 4 weeks (Group Ia, IIa, and IIIa) and 8 weeks (Group Ib, IIb, and IIIb).

Selenium-deficient diet

Selenium-deficient diet with inactivated Baker's yeast as a protein source was prepared in the laboratory itself according to the composition given by Burk [24]. The diet contained inactivated torula yeast (inactivated by autoclaving) 30%, sucrose 56.99%, corn oil 6.67%, mineral mix 5%, vitamin mix 1%, DL-methionine 0.3%, and vitamin E 0.04%. Se-adequate and -excess diets were prepared from Se-deficient diet by supplementing it with 0.2 ppm and 1 ppm of Se, respectively, as sodium selenite. After completion of diet-feeding schedule of 4 and 8 weeks, animals were sacrificed by cervical dislocation under anesthesia (50 mg/Kg body weight of Sodium Phenobarbital), testes were removed and used for various analyses.

Selenium estimation

Selenium levels in testis were estimated as previously described [25]. The method is based on the principle that Se in tissues on acid digestion is converted into selenous acid which on reaction with aromatic-o-diamines such as 2,3-diamine naphthalene (DAN) leads to the formation of 4,5-benzopiazselenol which displays brilliant lime-green fluorescence. In brief, 100 mg of testis tissue was acid digested in concentrated HNO_3 on a sand bath at approx. 100°C in digestion flasks fitted with long air condenser to prevent any Se vapor loss. A known amount of digest was reacted with aqueous solution of DAN (precleaned of impurities with cyclohexane). The product formed (4,5-benzopiaselenol) was extracted completely with cyclohexane and quantitated on fluorescence spectrophotometer (Perkin Elmer, USA) using 366 nm as excitation and 520 nm as emission wavelength. Sodium selenite was used as a standard for this assay.

Biochemical estimations

Tissue homogenates (10% w/v) were prepared in 50-mM Tris–HCl (pH 7.4) under ice-cold conditions. The homogenates were then centrifuged at 10,000 rpm for 30 min. The supernatant (post-mitochondrial fraction, PMF) thus obtained was collected for the biochemical estimations described below.

Se-dependent glutathione peroxidase activity

Activity of glutathione peroxidase (GSH-Px) was assayed by the coupled enzyme procedure with glutathione reductase using H_2O_2 as substrate [26]. The assay was carried out in testis PMF. The activity was expressed as micromoles of NADPH oxidized/min/mg protein. Total protein was estimated by the method of Lowry et al. [27].

Lipid peroxidation (LPO) assay

The levels of LPO were assayed according to the method of Wills [28]. Since malondialdehyde (MDA) is a degradation product of peroxidized lipids, the development of pink color with the absorption characteristics (absorption maxima at 532 nm) as TBA–MDA chromophore is taken as an index of the lipid peroxidation. For standard, a 2–10 nmol range of 1,1′,3,3′-tetraethoxypropane (TEP) was used, and for control, distilled water was used instead of the sample. MDA levels were expressed as nanomoles MDA/mg protein.

ROS estimation

Determination of ROS was based on the modified method of Driver et al. [29]. Testicular homogenates were prepared in ice-cold Locke's buffer (154 mM NaCl, 5.6 mM KCl, 3.6 mM $NaHCO_3$, 2.0 mM $CaCl_2$, 10 mM D-glucose, and 5 mM HEPES pH 7.4). The homogenates were kept at 21°C for 5 min. The reaction mixture containing 10 μM DCFH-DA and 5 mg tissue/ml was incubated for 15 min at room temperature (21°C) to allow the probe to be incorporated into any membrane-bound vesicles, and the diacetate groups cleaved by esterases. After another 30 min of incubation, the conversion of DCFH to the fluorescent product DCF was measured using fluorescence spectrophotometer with excitation at 485 nm and emission at 530 nm. Background fluorescence (conversion of DCFH to DCF in the absence of homogenate) was corrected by inclusion of parallel blanks. The relative difference in fluorescence intensity was taken as the measure of the amount of ROS in different treatment groups.

RNA isolation

Total RNA was isolated from mice testis using TRI-REAGENT (Mol Res. Centre, Inc, Ohio, USA). Fifty milligrams testis tissue from different treatment groups was homogenized in 0.5 ml of TRI-REAGENT using hand homogenizer in 1.5 ml polystyrene microfuge tubes. The samples were kept at room temperature for 5 min. Thereafter, 80 μl chloroform was added. This was mixed vigorously for about 15 s, and the homogenates were then kept

at room temperature for 10 min followed by centrifugation at 12,000 rpm for 15 min at 4°C. After the centrifugation, the upper colorless aqueous phase containing RNA was collected. In order to precipitate RNA, isopropanol was added and after mixing, the samples were kept at room temperature for 10 min. Thereafter, samples were spun at 12,000 rpm for 10 min at 4°C. RNA precipitate so obtained was washed by adding 75% ice-cold ethanol and spinning at 7500*g* at 5 min at 4°C. After removing the ethanol, the RNA pellet was briefly air-dried (not completely) and then dissolved in DEPC-treated water. Purity, integrity, and concentration of the isolated RNA were checked by taking absorbance at 260 and 280 nm and finding their ratios. Concentration of RNA was estimated by using $A_{260} = 1$=40 μg/ml.

Primer designing and synthesis for RT-PCR analysis

For the RT-PCR analysis, the DNA sequence for the following genes, i.e., p38, Bcl-2, caspase-3, and caspase-8 were searched from the computer data base. Primers for each of these genes were designed from the sequence data with the help of software "Gene Runner" and obtained as-synthesized from Sigma-Aldrich (USA). Length of the primers chosen was ~20 bp. Primer sequences designed for different genes are given in Table 1.

RT-PCR procedure

RT-PCR was done using specific primers for the respective genes. RT-PCR for *β*-actin was also done along with to rule out the experimental errors. QIAZEN one step RT-PCR kit was used for the purpose. Two micrograms of total RNA was used in RT-PCR reaction from different groups. To this, the following reagents were added as follows: 10 μl 5× Qiagen one step RT-PCR buffer, 2 μl dNTP mixture, 5 μl each of forward and reverse primers (10 μM stock), 2 μl enzyme mix, and 1 μl RNase inhibitor (1 U/μl). Finally, PCR grade RNase free water was added to make a total volume of 50 μl. The components were mixed with gentle vortex and centrifuged to collect all the components at the bottom of the tube. The PCR reaction was performed in the thermal cycler (Techne Ltd, England) using following conditions: RT reaction was performed at 50°C for 50 min and activation at 94°C for 15 min. PCR was followed by 35 cycles of 94°C (denaturation) for 45 s, 56°C (annealing) for 45 s, and 68°C (extension) for 1 min. Finally, the products were incubated at 68°C for 5 min to extend any incomplete single strands. In order to authenticate the results from RT-PCR (a semi-quantitative method) analysis, the analysis was initially carried out at 20, 25, 30, and 35 cycles for various genes. Progressive increase in products was obtained in all the cases and hence finally the RT-PCR was done with the samples at 35 cycles only.

Final PCR products formed were analyzed on 1.5% agarose gel electrophoresis, and densitometric analysis of the bands was done by Image J software (NIH, USA). Mean of four independent densitometric analyses of PCR product bands were determined for comparison of each analysis.

Western immunoblot analysis

Protein samples (60 μg) from each treatment group were separated on 12% SDS-PAGE. The separated proteins were electrophoretically transferred to PVDF membrane (Millipore, USA). Immunoblot was prepared using anti-mouse anti-p38 primary antibody and peroxidase-conjugated anti-rabbit IgG secondary antibody (Sigma-Aldrich). Diaminobenzedine (DAB) plus H_2O_2 detection system was used to develop the blot.

For preparation of cell lysate, testes were collected from the different treatment groups after completion of diet-

Table 1 Primer sequences

Gene	Primer		Reference	Product size
Bcl-2	Sense	5′ AGA GGG GCT ACG AGT GGG AT 3′	Levine et al. [44]	450 bp
	Antisense	5′ CTC AGT CAT CCA CAG GGC GA 3′		
Caspase 3	Sense	5′ AGT CAG TGG ACT CTG GGA TC 3′	Grimm et al. [45]	346 bp
	Antisense	5′ GTA CAG TTC TTT CGT GAG CA 3′		
β-actin	Sense	5′ ATC CGT AAA GAC CTC TAT GC 3′	Yamada et al. [46]	287 bp
	Antisense	5′ AAC GCA GCT CAG TAA CAG TC 3′		
p38	Sense	5′ TAT CCA CTC GGC GGG CAT CA 3′	NM011161	300 bp
	Antisense	5′ GTG CCC ACC ACC TCC ATG AT 3′		
Caspase 8	Sense	5′ TGC CCT CAA GTT CCT GTG CTT GGA 3′	Zender et al. [47]	228 bp
	Antisense	5′ GGA TGC TAA GAA TGT CAT CTC C 3′		

feeding schedule of 4 and 8 weeks. Total lysates were prepared in fresh ice-cold protein lysis buffer (50 mM Tris pH 7.5, 150 mM NaCl, 0.1% NP-40, 50 mM NaF, 1 mM Na_3VO_3, and 1 mM PMSF). The extracts were cleared by centrifugation at 440*g* for 10 min at 4°C. The supernatants were collected, and protein concentration was determined individually by method of Lowry et al. [27].

Immunohistochemical localization studies

Paraffin sections of 6 μm thickness of mice testis were deparaffinized in two fresh changes of xylene for 30 min each. The sections were then gradually hydrated and finally brought to water. Endogenous peroxidase activity was blocked by incubation with 3% H_2O_2 for 30 min at 37°C. The non-specific staining was blocked by incubating sections with 2% BSA in phosphate buffer saline (PBS 10 mM, pH 7.2). The sections were then incubated with polyclonal antibody against p38 (Sigma-Aldrich; 1:8000) in a moist chamber for 1h at 37°C. After incubation, the sections were washed in PBS, PBS tween (PBS with 0.05% tween-20) and PBS successively for 5 min each. The sections were then incubated with peroxidase-labeled anti-rabbit IgG (1:500) for 1h. Sections were washed again in the same manner as described above, and the reaction product was developed using diaminobenzidine (DAB) and H_2O_2. Reaction was terminated by washing with distilled water, and then sections were mounted in glycerol jelly.

Microscopy and data analysis

Sections were viewed and photographed with a Leica Optiphot microscope to which was attached a Leica Digital camera. For each testicular cross section, all cross-sectional tubular profiles ($\sim$100–150) were counted.

TUNEL assay for detection of apoptotic germ cells

Terminal deoxynucleotidyl transferase-mediated dUTP-biotin nick end-labeling (TUNEL) was carried for in situ visualization of DNA fragmentation indicative of apoptosis using in situ cell-death detection kit (Roche Diagnostics, Germany) on 7-micron-thick paraffin-embedded testis sections on glass slides. After proteinase K treatment, slides were treated with TUNEL reaction mixture containing label solution and enzyme solution. Thus 3′-OH DNA ends were labeled with biotin conjugated dUTP and detected with avidin conjugate. For the negative control, only label solution without any enzyme solution was added. For the positive control, 50 μl DNase I (1,500 U/ml) was added for 10 min at 25°C, and then TUNEL reaction mixture was added.

Statistical analysis

The differences between Means ± Standard Deviations (SD) for control and treated groups were examined by using the Student's *t*-test for unpaired values. Statistical difference of *t*-value at the level of 0.05 or less was considered significant.

Results

Glutathione peroxidase activity

A significant decrease in the activity of GSH-Px was observed in both Se-deficient groups, Ia and Ib, when compared with Se-adequate group IIa and IIb, respectively. On the other hand, significant increase was observed in Se-excess groups, IIIa and IIIb, as compared with the respective Se-adequate groups IIa and IIb. The data are shown in Table 2, which further strengthens the observations of establishment of Se status and the prevalence of oxidative stress conditions in the testicular compartment.

Lipid peroxidation

Significant increase in lipid peroxidation was observed in Se-deficient groups, Ia and Ib, as compared with their respective Se-adequate groups, IIa and IIb, after 4 and 8 weeks (Table 2). In Se-excess group, significant increase in lipid peroxidation was observed in group IIIa after 4 weeks of diet feeding. This increased more significantly at longer duration of 8 weeks in group IIIb compared with the respective Se-adequate group IIb.

ROS generation

As shown in Table 2, significant increase in ROS generation was observed in group Ia which became highly significant at 8 weeks (group Ib) as compared with groups, IIa and IIb. Similar increase in the generation of ROS was observed in groups, IIIa and IIIb.

mRNA expression of p38, Bcl-2, caspase 3, and caspase 8

Alterations in the mRNA expression of p38, Bcl-2, caspase 3, and caspase 8 following Se-induced oxidative stress were analyzed and are shown in Figs. 1, 2, 3, and 4a. Significant increase in the mRNA expression of p38 was observed under the conditions of Se-deficiency and Se-excess as compared with the respective Se-adequate group. However, this increase was more prominent in the Se-deficient group. Moreover, the increase was more

Table 2 Effect of modulation in selenium status on glutathione peroxidase activity, lipid peroxidation, and ROS generation

	Se deficient Gp Ia	Se adequate Gp IIa	Se excess Gp IIIa	Se deficient Gp Ib	Se adequate GpIIb	Se excess Gp IIIb
Selenium estimation (μg Se/g tissue)	0.562 ± 0.015***	0.723 ± 0.018	0.842 ± 0.04***	0.429 ± 0.017***	0.701 ± 0.016	0.927 ± 0.03***
Glutathione peroxidase (μmoles of NADPH oxidized/min/mg protein)	85.87 ± 1.12***	119.23 ± 1.60	148.57 ± 3.27**	47.85 ± 1.10***	114.46 ± 3.69	132.17 ± 1.43***
Lipid peroxidation (n moles of MDA/mg protein)	4.60 ± 0.27***	2.23 ± 0.42	4.04 ± 0.14***	6.32 ± 0.92***	3.42 ± 0.11	4.88 ± 0.58***
ROS production (relative fluorescent intensity of DCF)	40.88 ± 2.12***	14.21 ± 1.10	33.23 ± 1.43***	86.40 ± 5.42***	30.42 ± 3.26	67.01 ± 4.03***

The values are mean ± SD of six independent observations. *, **, *** represent $P < 0.05$, $P < 0.01$, $P < 0.001$, respectively

pronounced at the 8 weeks' interval as compared with the 4 weeks' interval.

The reverse trend was observed in the mRNA expression of Bcl-2 as shown in Fig. 4a. There was a highly significant reduction in the mRNA expression of Bcl-2 in Se-deficient group and -excess group. The decrease was more pronounced at 8 weeks' interval in both the cases. Moreover, the decrease in deficient group was greater as compared with the excess group at both the treatment intervals.

There was a significant increase in the mRNA expression of caspase 3 and caspase 8 in Se-deficient and -excess groups at both the treatment intervals as shown in Figs. 2a and 3a; as compared with the adequate-diet-fed group. The increase in the mRNA expression was more pronounced in the deficient group at both the treatment intervals as compared to the excess-diet-fed group. Densitometric analysis (Figs. 1b, 2b, 3b, and 4b) of the bands obtained clearly demonstrates that the increase and decrease in the band intensity were statistically significant in all the cases.

The results obtained confirm the activation of apoptotic machinery in Se-stressed groups as seen by the activation of caspase 8: the major apoptosis initiator caspase; and by the activation of caspase 3: the major effector caspase. The activation of apoptotic pathway was further confirmed by the decrease observed in the expression of Bcl-2: an anti-apoptotic protein. The involvement of p38 in the execution of apoptosis was confirmed by its activation concomitant with the activation of caspases 3 and caspases 8 and suppression of Bcl-2, as observed in this study.

Western immunoblot analysis

In order to ascertain whether activation of mRNA expression of p38 under Se status also led to an increase in the protein product, Western immunoblot analysis for p38 MAPK was done as shown in Fig. 5a,b. The results obtained clearly demonstrate significant increase in the protein expression of p38 under Se-deficient and Se-excess conditions as compared to the respective Se-adequate conditions. However, this increase was more prominent in the Se-deficient group. Also, the increase was more pronounced at the 8 weeks' interval as compared to the 4 weeks' interval. The results obtained demonstrate that an increase in the mRNA expression finally caused an increased protein expression under Se-stressed conditions.

Immunohistochemical localization studies

In order to establish whether activation of p38 may be responsible for activation and execution of apoptotic cell death under Se-stressed conditions, we performed p38

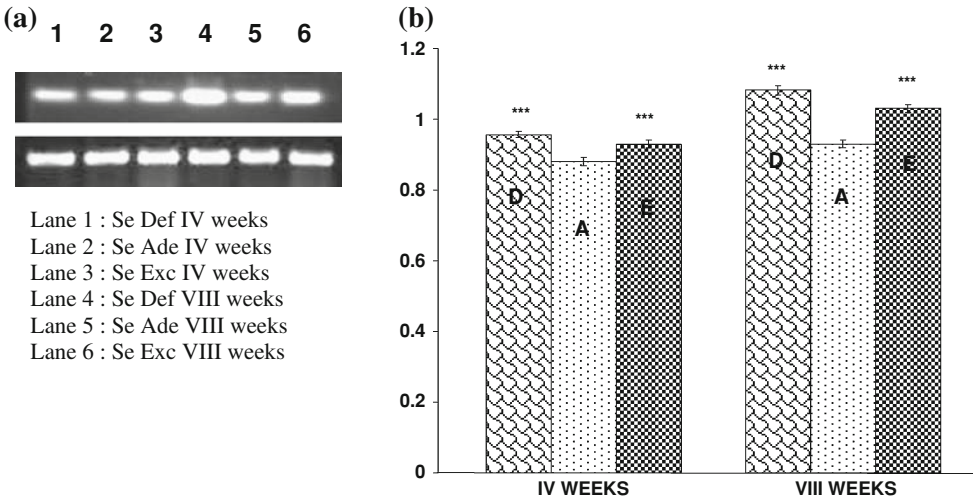

Fig. 1 Effect of modulation in selenium status on the mRNA expression of p38 (**a**) and its densitometric analysis (**b**). Lane I—Se deficient (4 weeks), Lane II—Se adequate (4 weeks), Lane III—Se excess (4 weeks), Lane IV—Se deficient (8 weeks), Lane V—Se adequate (8 weeks), Lane VI—Se excess (8 weeks). The values are mean ± SD of three independent observations. *, **, *** represent $P < 0.05$, $P < 0.01$, $P < 0.001$, respectively

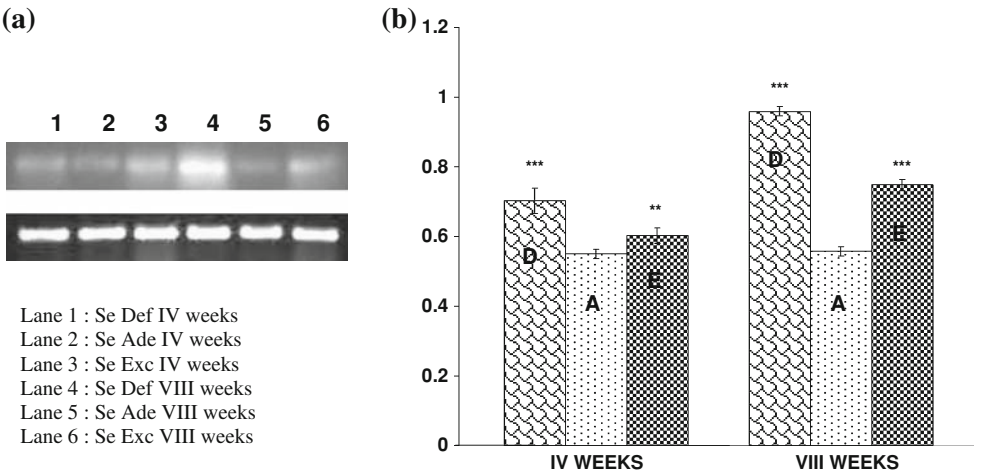

Fig. 2 Effect of modulation in selenium status on the mRNA expression of Caspase 3 (**a**) and its densitometric analysis (**b**). Lane I—Se deficient (4 weeks), Lane II—Se adequate (4 Weeks), Lane III—Se excess (4 weeks), Lane IV—Se deficient (8 weeks), Lane V—Se adequate (8 weeks), Lane VI—Se excess (8 weeks). The values are mean ± SD of three independent observations. *, **, *** represent $P < 0.05$, $P < 0.01$, $P < 0.001$, respectively

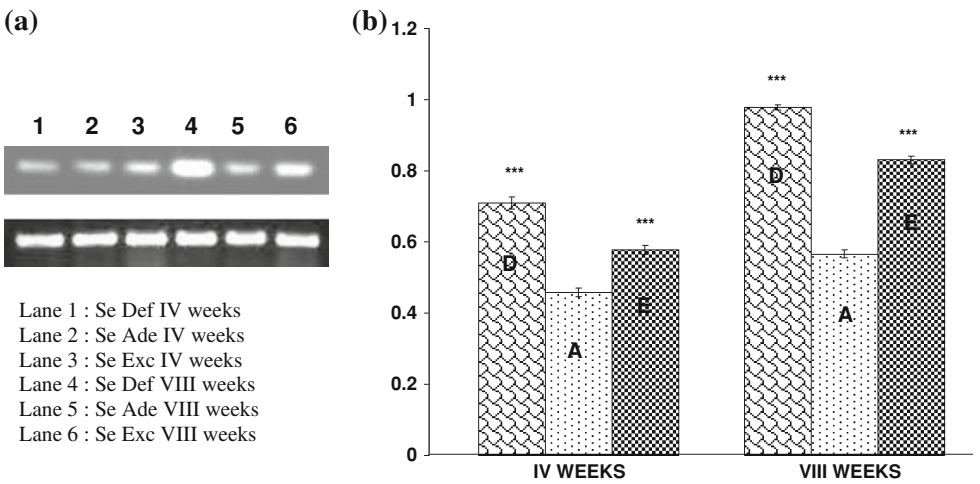

Fig. 3 Effect of modulation in selenium status on the mRNA expression of Caspase 8 (**a**) and its densitometric analysis (**b**). Lane I—Se deficient (4 weeks), Lane II—Se adequate (4 weeks), Lane III—Se excess (4 weeks), Lane IV—Se deficient (8 weeks), Lane V—Se adequate (8 Weeks), Lane VI—Se excess (8 weeks). The values are mean ± SD of three independent observations. *, **, *** represent $P < 0.05$, $P < 0.01$, $P < 0.001$, respectively

immunostaining in all the treatment groups. It was observed that all the cell types stained positive for p38 MAPK, but the frequency of each cell type varied under different Se statuses during 4–8 weeks (Figs. 6, 7).

Spermatogonia

There was an increase in the number of spermatogonia staining positive for p38 in Se-deficient and Se-excess

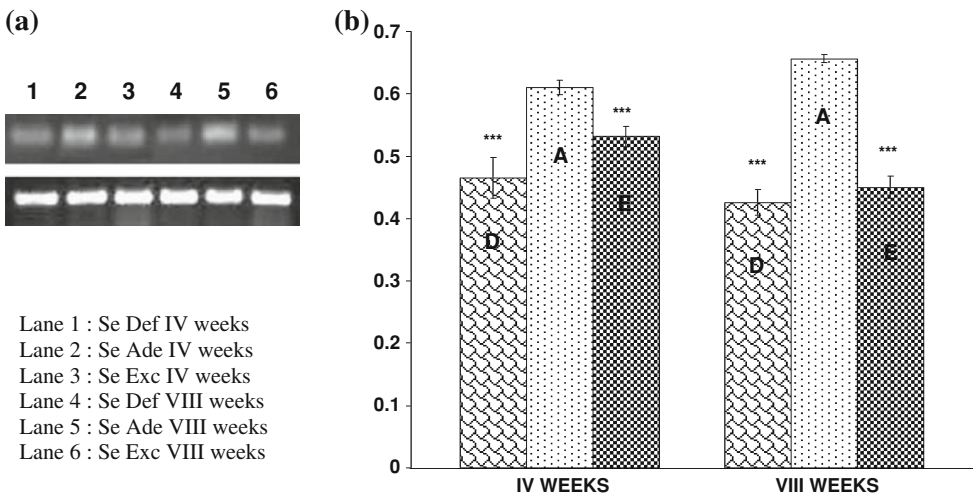

Fig. 4 Effect of modulation in selenium status on the mRNA expression of Bcl-2 (**a**) and its densitometric analysis (**b**). Lane I—Se deficient (4 weeks), Lane II—Se adequate (4 weeks), Lane III—Se excess (4 weeks), Lane IV—Se deficient (8 weeks), Lane V—Se adequate (8 weeks), Lane VI—Se excess (8 weeks). The values are mean ± SD of three independent observations. *, **, *** represent $P < 0.05$, $P < 0.01$, $P < 0.001$, respectively

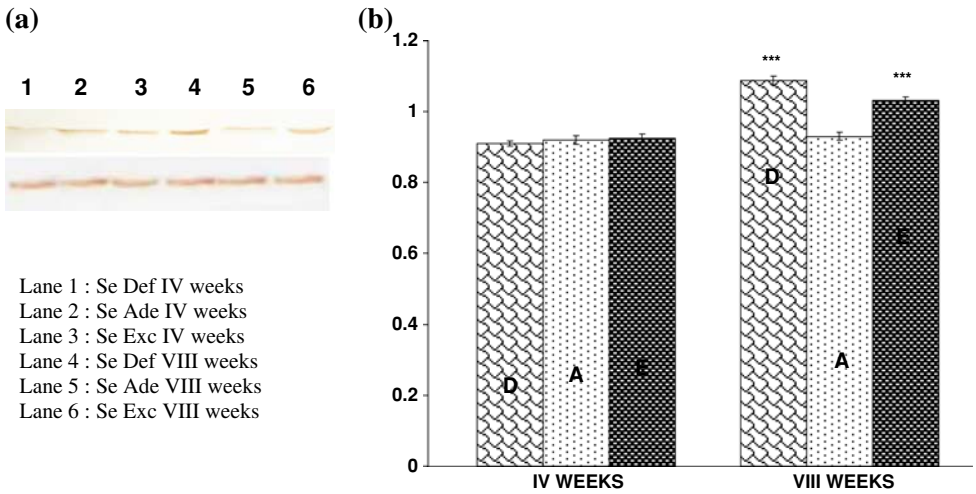

Fig. 5 Effect of modulation in selenium status on the protein expression of p38 (**a**) and its densitometric analysis (**b**). Lane I—Se deficient (4 weeks), Lane II—Se adequate (4 weeks), Lane III—Se excess (4 weeks), Lane IV—Se deficient (8 weeks), Lane V—Se adequate (8 weeks), Lane VI—Se excess (8 weeks). The values are mean ± SD of three independent observations. *, **, *** represent $P < 0.05$, $P < 0.01$, $P < 0.001$, respectively

groups as compared with the respective Se-adequate groups at 4 weeks' interval. However, the increase was highly pronounced in the Se-deficient group at 8 weeks' interval as compared with the adequate group, whereas the Se-excess group showed a lesser increase.

Primary spermatocyte

A similar trend for p38 immunostaining was observed in case of primary spermatocytes. There was an increase in the number of p38 positive cells in Se-deficient and Se-excess groups as compared with their respective Se-adequate groups at both the treatment intervals.

Round spermatid

Round spermatids also stained positive for p38, and the trend was similar to that observed in the case of primary spermatocytes.

Elongated spermatids

Immunostaining for p38 in the elongated spermatids was altogether different. The staining followed the same trend as in the case of primary spermatocyte and round spermatid for the 4 weeks' interval, but in the 8 weeks' duration, the p38 positive elongated spermatids were found to be maximum in Se-adequate group, followed by the Se-excess group, and as found to be the least in Se-deficient group at 8 weeks' interval.

TUNEL assay

TUNEL assay was used to identify and characterize apoptotic germ cells following induction of oxidative stress by Se. The frequency of apoptotic germ cells was more in the testicular sections of Se-deficient and Se-excess animals (Fig. 8a, c) as compared with the Se-adequate-

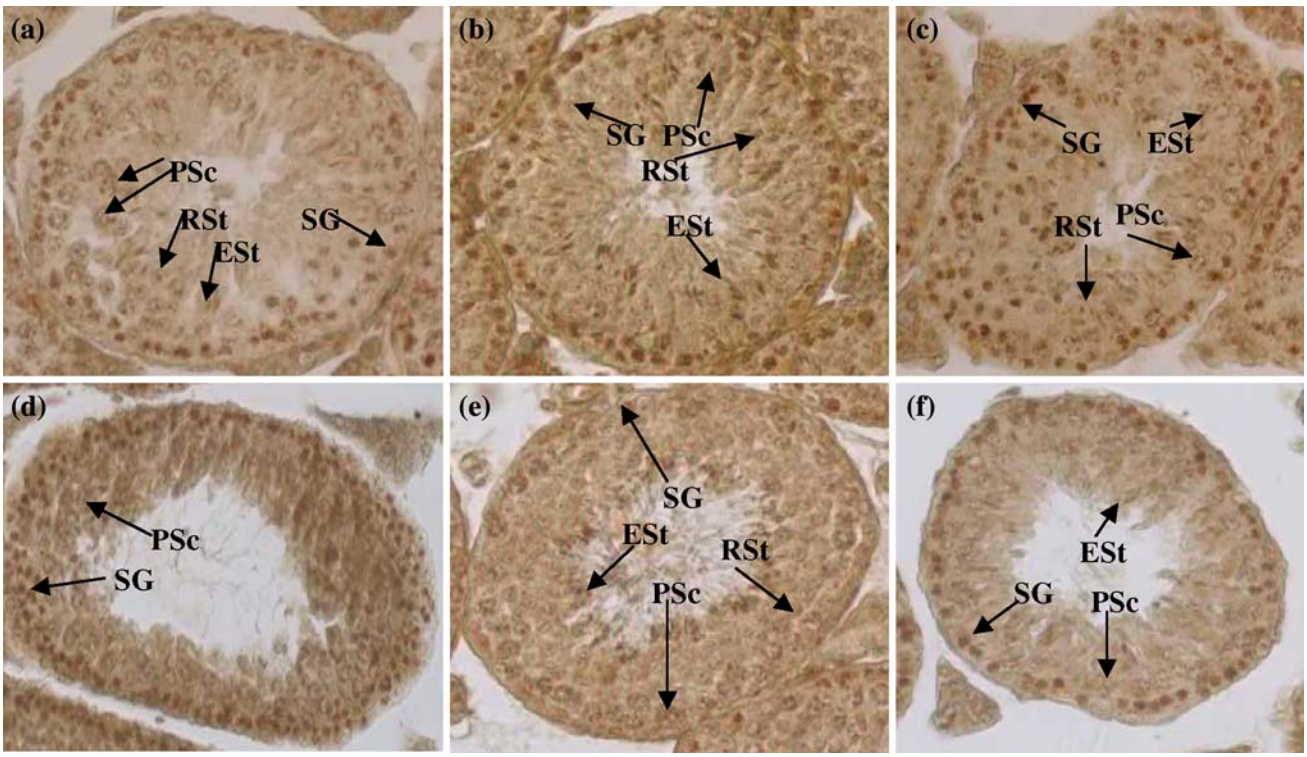

Fig. 6 Photomicrograph showing effect of modulation in selenium status on p38 immunostaining in testis paraffin sections of mice fed respective diet for 4 weeks and 8 weeks. **a** Se deficient (IV weeks), **b** Se adequate (IV weeks), **c** Se excess (IV weeks), **d** Se deficient (VIII weeks), **e** Se adequate (VIII weeks), **f** Se excess (VIII weeks). *SG* Spermatogonia, *PSc* Primary spermatocytes, *RSt* Round spermatid, *ESt* Elongated spermatid

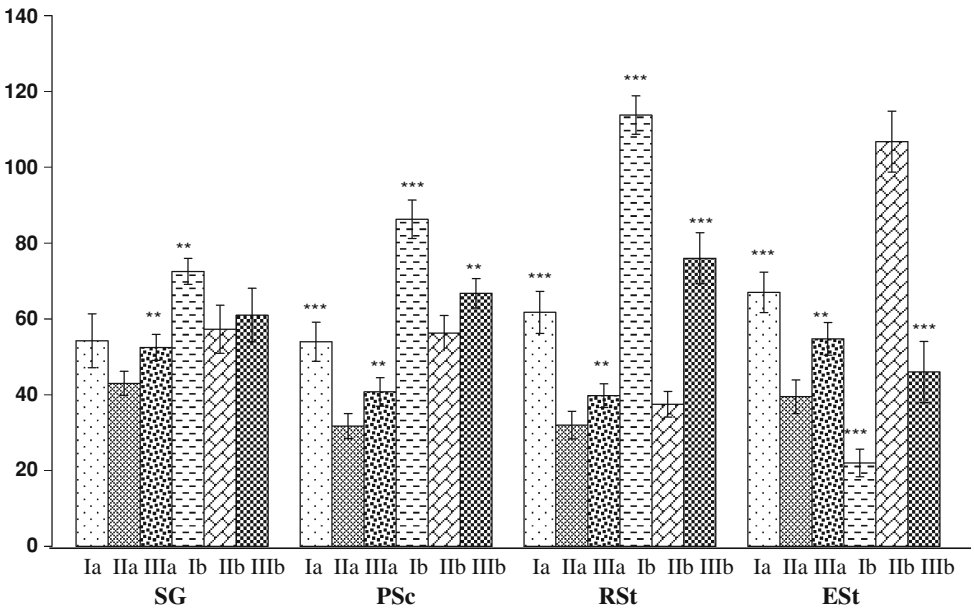

Fig. 7 Graphical representation of p38 immunokinetics in various testicular cell populations

group (Fig. 8b). Spermatogonial cell populations were found to be maximally apoptotic in both Se-deficient as well as Se-excess groups. However, in the Se-deficient animals, there was also a simultaneous increase in the TUNEL-positive elongated spermatids (Fig. 8a) compared with the Se-adequate group, where no such DNA damage was observed except in the spermatogonial cell population (Fig. 8b). Apoptosis in the Se-excess group was also noticed by condensation of nuclei in the spermatogonia, round, and elongated spermatids (Fig. 8c).

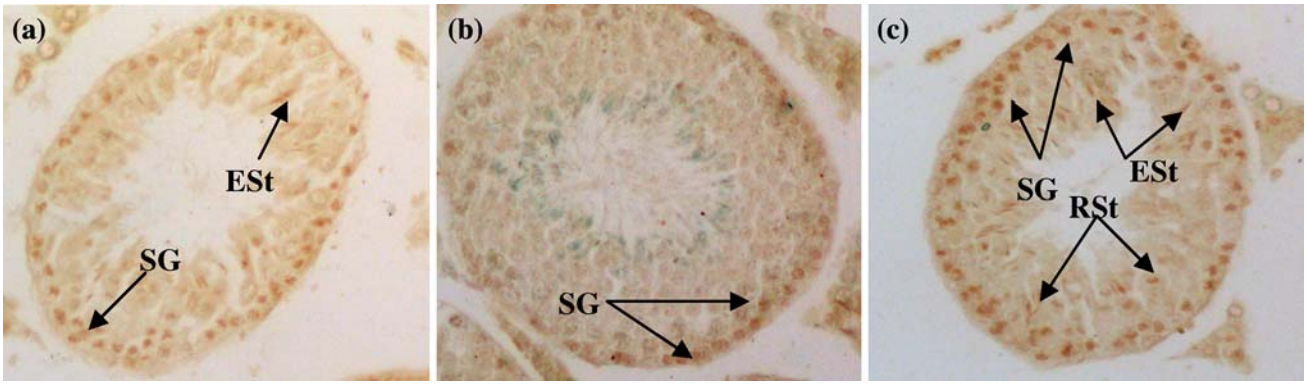

Fig. 8 Photomicrograph showing TUNEL staining in testis paraffin sections of mice fed respective diet for 8 weeks. **a** Se deficient (VIII weeks), **b** Se adequate (VIII weeks), **c** Se excess (VIII weeks). *SG* Spermatogonia, *RSt* Round spermatid, *ESt* Elongated spermatid

Discussion

In this study, we evaluated the signaling pathway during testicular apoptosis triggered by Se-deficiency and Se-excess conditions. Our results demonstrate that initiation of testicular apoptosis was preceded by p38 MAPK activation and generation of ROS. These events are accompanied by suppression of antiapoptotic Bcl-2 and activation of caspase 3 and caspase 8.

In order to address the first phase of this study, the establishment of Se status in the animals under study was evaluated. A decrease in Se levels in Se-deficient group and an increase in the Se-excess group at both the treatment intervals confirmed the establishment of Se status in the animals, as also reported elsewhere in a previous study from our laboratory [30].

GSH-Px activity decreased in Se-deficient groups at both the treatment intervals. Decreased Se levels [30] concomitant with the decrease in GSH-Px activity might contribute to building up of oxidative stress in Se-deficient group at both 4 and 8 weeks' interval. In Se-excess group, increase in GSH-Px activity was observed at 4 weeks' interval, but the activity of GSH-Px ceased to increase further as observed at 8 weeks' interval. Other studies have reported that various homeostatic processes control the level of GSH-Px, and the higher intake of Se beyond the nutritionally adequate level does not elicit any further increase in enzyme activity [31].

Lipid peroxidation was found to be increased in Se-deficient and -excess groups. The increase in lipid peroxidation in Se-deficient group can be explained on the basis of decreased levels of GSH-Px. Surai et al. (1998) [32] reported that this enzyme represents more than 75% of total enzyme activity in spermatozoa. As a result of the loss of GSH-Px activity, peroxides accumulate and alter the redox environment of the cells. In Se-excess group, increased LPO could be attributed to the ability of selenite to form a highly reactive species GSSe—a selenopersulfide [33], which generates free radical, superoxide, as well as other ROS.

The increased generation of ROS was also evidenced in this study in both, Se-deficient and -excess conditions which further supports the existence of oxidative stress conditions in the testicular compartment. There has been accumulating evidence supporting a role for ROS as second messengers that modulate gene transcription [34]. Thus, it could be concluded that modulation in Se status leads to building up of oxidative stress through generation of ROS.

These elevated levels of ROS may affect stress-responsive signal transduction cascades, including MAPKs pathways. The previous study [15] conducted in our lab have demonstrated that elevated levels of ROS under Se-deficient and -excess conditions affect the reproductive potential of mice, finally leading to decrease in sperm number, motility, and percentage fertility, through inactivation of transcription factor, AP-1. The AP-1 is the downstream target for MAPKs including p38. Further, various studies report that p38 pathway is responsive to ROS and involved in apoptosis. This aspect was dealt with in the next phase of the study where it was explored to conclude whether the existing oxidative stress in the testis in this study modulated the expression of p38 MAPK which finally could culminate in apoptosis.

Indeed, in this study, we found increased expression of p38 MAPK under Se-deprived and Se-excess conditions. This was more pronounced in the 8 weeks' interval and also in case of Se deficiency as evidenced by the mRNA expression and protein expression. In order to follow the cell specific expression of p38 in the testicular compartment, which would help elucidate the role of p38 in the progression of the various spermatogenic stages involving the apoptotic process, immunohistochemical localization studies for p38 were carried out. All the tubules belonging

to stage VI–VIII were taken into account, in which the spermatogenic process is toward completion, and the stages of spermiation are about to start. The tubules below stage VI were not taken into account because they correspond to the developing stages in the progression of spermatogenesis.

It was observed that p38 MAPK immunostaining was localized in all spermatogenic stages, starting from spermatogonia (mitotic stage) to the spermatid (meiotic stage). This localization of p38 in all the spermatogenic stages underlies its importance for the proper progression of spermatogenesis. The immunostaining was highly prominent in all the cell types in Se-deficient and Se-excess groups at 4 weeks' interval as compared with control in which immunostaining was less intense (as explained by the quantitative analysis). However, the localization was less pronounced in Se-excess group as compared to Se-deficient group. As we moved to the localization of p38 in the 8 weeks' interval, it was observed that the number of spermatogonia and primary spermatocytes staining positive for p38 in Se-deficient group increased in number, confirming a highly pronounced expression. As the testicular histoarchitecture is highly altered in Se-deficient group at the 8 weeks' interval, which results in loss of round and elongated spermatids, we did not find enough immunostained cells comprising this population. Tubules from 8 weeks Se-adequate group showed all the cell types staining positive for p38 MAPK. Results similar to Se-deficient group were also observed in Se-excess group, but here the cells staining positive for p38 MAPK decreased in number from the spermatogenic to the spermatocyte cell types, and decreased further up to the spermatid stages. These results could also be explained on the basis of alteration in histoarchitecture in Se-excess group which resulted in loss of cell population.

However, the phosphorylation status of p38 MAPK requres to be confirmed by using phosphorylated antibodies, which could not be done at that time. Thus, in order to confirm the increased expression of p38 MAPK in this study by mRNA expression, protein expression, and immunohistochemical localization studies, a further study carried out to explore the involvement of p38 MAPK in the culmination of apoptosis by the activation and deactivation of various apoptotic factors.

It is well established that supply of sufficient amounts of Se to the testis has priority over the supply to other tissues, and that supply of this micronutrient to the testis is highly regulated. As a potent antioxidant, it constituted the essential component of GSH-Px which catalyses the degradation of peroxides and helps maintain the redox status of the cells [35]. Although Se is an essential trace element for normal cell functions of all the mammalian species, toxic effects of the high selenite concentrations have been reported in both in vivo and in vitro studies. Morevoer, it has been suggested that Se cytotoxicity is related to the generation of free radicals that induces apoptosis.

The p38 MAPK pathway has been implicated in apoptotic response of various cell systems exposed to a variety of environmental stresses and inflammatory signals [36]. Thus, the signal for p38 activation most likely emanated from the stress generated by the dramatic loss of this element in Se-deficient conditions and by the increase in the level of ROS in Se-excess group. These data indicate that p38 MAPK plays a role in testicular apoptosis induced by Se-deficient and Se-excess conditions.

Consistent with the activation of p38 in the Se-deficient and -excess groups was the suppression of Bcl-2 and activation of caspase 3 and caspase 8 in the respective groups. One intriguing possibility is that p38 MAPK could induce apoptosis through the activation of the cytochrome c-mediated death pathway which finally culminates in the activation of the executioner caspase 3. Various studies indicate that the caspase 3 is a key protease mediating apoptosis. The activation of caspase 3 in Se-deficient and -excess conditions as observed in our study supports the involvement of cytochrome c mediated death pathway. This is consistent with the previous findings indicating the involvement of the mitochondria-dependent intrinsic pathway signaling in testicular germ cell death triggered by heat stress [37].

An increase in the mRNA expression of the caspase 8 was also seen in Se-deficient and Se-excess groups. It is well established that the caspase 8 participates in the regulation of the cytochrome c during the apoptotic process [38]. It has been shown that MAPK family members have a role in activating caspase cascades [39]. Recently, Bhattacharyya et al. [40] reported that p38 MAPK signaling was linked to the activation of the caspase 8, which has been reported to be an important component of the Fas receptor death-inducing signaling complex (DISC), and activation of caspase-8 in the DISC results in the activation of downstream caspases and the cleavage of cytosolic substances such as Bid, a BH3 domain-only protein [19]. These findings suggested that p38 MAPK signaling plays a crucial role in the activation of caspase 8.

The Bcl-2 family of proteins governs the mitochondria dependent pathway of apoptosis [41]. Bcl-2 has been shown to prevent apoptosis [42]. The mRNA expression of Bcl-2 in our study clearly shows that induction of testicular apoptosis is associated with decrease in Bcl-2 levels—as observed in Se-deficient and -excess groups.

Further, apoptotic cells observed in our study in Se-deficient and -excess groups at 8 weeks can also be explained on the basis of caspase 3 activation. Among the effector caspases, activated CP3 appears to induce activation of caspase-activated deoxyribonuclease (CAD; also called DNA fragmentation factor-40 or caspase-activated

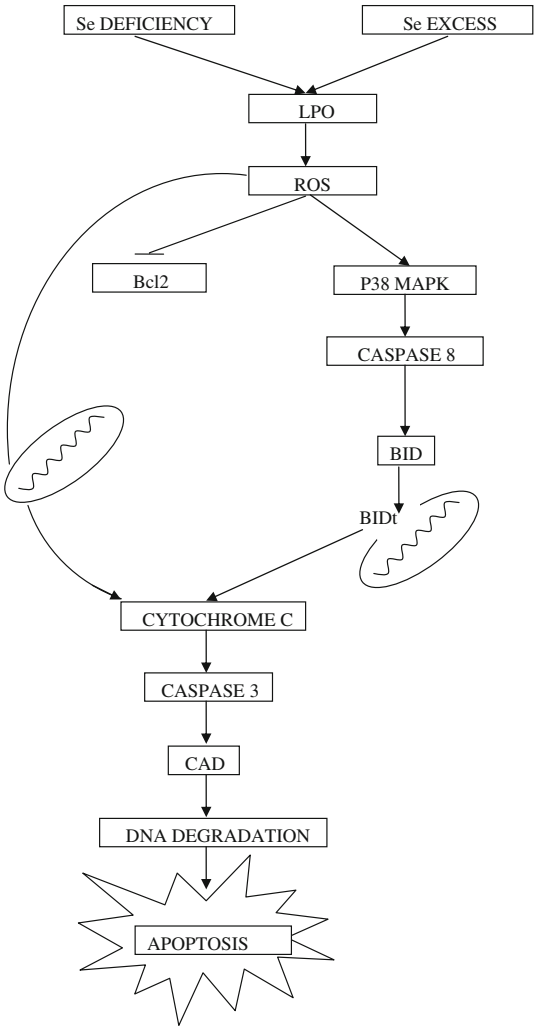

Fig. 9 Proposed pathway delineating the molecular mechanism behind selenium status induced apoptosis involving p38 MAPK and ROS

nuclease), which is integrally involved in degrading DNA. Therefore, CP3 appears to be the most important among them as it executes the final disassembly of the cell by generating DNA strand breaks [43]. Sperm DNA fragmentation was prevalent in fractions of sperm with positive immunostaining for active CP3, suggesting a relationship between them [20].

In order to summarize as depicted in Fig. 9, this study demonstrates that ROS, generated by the deficiency and excess of the trace element Se, finally leads to the activation of p38 and caspase 8. The activated p38 and caspase 8 then leads to the activation of caspase 3. This activates caspase 3, then degrades DNA, and executes the final disassembly of cell culminating in apoptosis.

Acknowledgment The authors acknowledge the financial support provided by Life Science Research Board, DRDO, Govt of India, New Delhi (India).

References

1. Borek C, Ong A, Mason H, Donahue L, Biaglow JE (1986) Selenium and vitamin E inhibit radiogenic and chemically induced transformation in vitro via different mechanisms. Proc Natl Acad Sci USA 83:1490–1494. doi:10.1073/pnas.83.5.1490
2. Zhuang S, Demirs JT, Kochevar IE (2000) p38 Mitogen-activated protein kinase mediates Bid cleavage, mitochondrial dysfunction, and caspase-3 activation during apoptosis induced by singlet oxygen but not by hydrogen peroxide. J Biol Chem 275(34): 25939–25948. doi:10.1074/jbc.M001185200
3. Behne D, Hilmert H, Scheid S, Gessner H, Elger W (1988) Evidence for specific selenium target tissues and new biologically important selenoproteins. Biochim Biophys Acta 966(1):12–21
4. Shen HM, Yang DF, Ong DN (1999) Induction of oxidative stress and apoptosis in sodium selenite-treated human hepatoma cells (HepG2). Int J Cancer 81:820–828. doi:10.1002/(SICI)1097-0215(19990531)81:5<820::AID-IJC25>3.0.CO;2-F
5. Sundaram N, Pahwa AK, Ard MD, Lin N, Perkins E, Bowles AP Jr (2000) Selenium causes growth inhibition and apoptosis in human brain tumor cell lines. J Neurooncol 46:125–133. doi:10.1023/A:1006436326003
6. Redman C, Xu MJ, Peng YM, Scott JA, Payne C, Clark LC, Nelson MA (1997) Involvement of polyamines in selenomethionine induced apoptosis and mitotic alterations in human tumor cells. Carcinogenesis 18:1195–1202. doi:10.1093/carcin/18.6.1195
7. Rayman MP (2000) The importance of selenium to human health. Lancet 356:233–241. doi:10.1016/S0140-6736(00)02490-9
8. Chandra J, Samali A, Orrenius S (2000) Triggering and modulation of apoptosis by oxidative stress. Free Radic Biol Med 29:323–333. doi:10.1016/S0891-5849(00)00302-6
9. Dumont A, Hehner SP, Hofmann TG, Ueffing M, Droge W, Schmitz ML (1999) Hydrogen peroxide-induced apoptosis is CD95-independent, requires the release of mitochondria-derived reactive oxygen species and the activation of NF-κB. Oncogene 18:747–757. doi:10.1038/sj.onc.1202325
10. Wang X, Sharma RK, Sikka SC, Thomas AJ Jr, Falcone T, Agarwal A (2003) Oxidative stress is associated with increased apoptosis leading to spermatozoa DNA damage in patients with male factor infertility. Fertil Steril 80:531–535. doi:10.1016/S0015-0282(03)00756-8
11. Schulze-Osthoff K, Ferrari D, Los M, Wesselborg S, Peter ME (1998) Apoptosis signaling by death receptors. Eur J Biochem 254:439–459. doi:10.1046/j.1432-1327.1998.2540439.x
12. Marshall CJ (1994) MAP kinase kinase kinase, MAP kinase kinase and MAP kinase. Curr Opin Genet Dev 4:82–89. doi:10.1016/0959-437X(94)90095-7
13. Kyriakis JM, Avruch J (1990) pp54 microtubule-associated protein 2 kinase, A novel serine/threonine protein kinase regulated by phosphorylation and stimulated by poly-L-lysine. J Biol Chem 265:17355–17363
14. Lee JC, Laydon JT, McDonnell PC, Gallagher TC, Kumar S, Green D et al (1994) A protein kinase involved in the regulation of inflammatory cytokine biosynthesis. Nature 372:739–746. doi:10.1038/372739a0
15. Shalini S, Bansal MP (2005) Role of selenium in regulation of spermatogenesis: involvement of activator protein 1. Biofactors 23:151–162. doi:10.1002/biof.5520230304
16. Aoshiba K, Yasui S, Hayashi M, Tamaoki J, Nagai A (1999) Role of p38-mitogen-activated protein kinase in spontaneous apoptosis of human neutrophils. J Immunol 162:1692–1700
17. Raff M (1998) Cell suicide for beginners. Nature 396:119–122. doi:10.1038/24055
18. Thornberry NA, Lazebnik Y (1998) Caspases: enemies within. Science 281:1312–1316. doi:10.1126/science.281.5381.1312

19. Muzio M, Chinnaiyan AM, Kischkel FC, O'Rourke K, Shevchenko A, Ni J et al (1996) FLICE, a novel FADD-homologous ICE/CED-3-like protease, is recruited to the CD95 (Fas/APO-1) death-inducing signaling complex. Cell 85:817–827. doi:10.1016/S0092-8674(00)81266-0
20. Choi WS, Eom DS, Han BS, Kim WK, Han BH, Choi EJ et al (2004) Phosphorylation of p38 MAPK induced by oxidative stress is linked to activation of both caspase-8- and -9-mediated apoptotic pathways in dopaminergic neurons. J Biol Chem 279:20451–20460. doi:10.1074/jbc.M311164200
21. Boesen-de Cock JG, Tepper AD, de Vries E, van Blitterswijk WJ, Borst J (1999) Common regulation of apoptosis signaling induced by CD95 and the DNA-damaging stimuli etoposide and γ-radiation downstream from caspase-8 activation. J Biol Chem 274:14255–14261. doi:10.1074/jbc.274.20.14255
22. Reed JC (1994) Bcl-2 and the regulation of programmed cell death. J Cell Biol 124:1–6. doi:10.1083/jcb.124.1.1
23. Rodriguez I, Ody C, Araki K, Garcia I, Vassalli P (1997) An early and massive wave of germinal cell apoptosis is required for the development of functional spermatogenesis. EMBO J 16:2262–2270. doi:10.1093/emboj/16.9.2262
24. Burk RF (1987) Production of selenium deficiency in rat. Methods Enzymol 143:307–313. doi:10.1016/0076-6879(87)43058-9
25. Hasunuma R, Ogawi T, Kawaniska Y (1982) Fluorometric determination of selenium in nanogram amounts in biological materials using 2,3-diaminonaphthalene. Anal Biochem 126:242–245. doi:10.1016/0003-2697(82)90510-3
26. Paglia DE, Valentine WN (1967) Studies on the quantitative and qualitative characterization of erythrocyte glutathione peroxidase. J Lab Clin Med 70:158–168
27. Lowry OH, Rosebrough NJ, Farr AL, Randall RJ (1951) Protein measurement with Folin phenol reagent. J Biol Chem 193:265–275
28. Wills ED (1966) Mechanisms of lipid peroxide formation in animal tissues. Biochem J 99(3):667–676
29. Driver AS, Rao P, Kodavanti S, Mundy WR (2000) Age-related changes in the reactive oxygen species production in rat brain homogenates. Neurotoxicol Teratol 22:175–181. doi:10.1016/S0892-0362(99)00069-0
30. Shalini S, Bansal MP (2007) Alterations in selenium status influences reproductive potential of male mice by modulation of transcription factor NFκB. Biometals 20:49–59. doi:10.1007/s10534-006-9014-2
31. Hafeman DG, Sunde RA, Hoekstra WG (1974) Effect of dietary selenium on erythrocyte and liver glutathione peroxidase in the rat. J Nutr 104:580–587
32. Surai P, Kostjuk L, Wishart G, Macpherson A, Speake B, Noble R et al (1998) Effect of vitamin E and selenium supplementation of cockerel diets on glutathione peroxidase activity and lipid peroxidation susceptibility in sperm, testes and liver. Biol Trace Elem Res 64:119–132. doi:10.1007/BF02783329
33. Shen HM, Yang CF, Liu J, Ong CN (2001) Superoxide radical initiated apoptotic signaling pathway in selenite treated HEPR2 cells: mitochondria serve as the main target. Free Radic Biol Med 30:9–21. doi:10.1016/S0891-5849(00)00421-4
34. Sen CK, Packer L (1996) Antioxidant and redox regulation of gene transcription. FASEB J 10:709–720
35. Spallholz JE (2001) Selenium and the prevention of cancer. Part II: mechanism for the carcinostatic activity of Se compounds, Bull STDA: 1–12
36. Tamagno E, Robino G, Obbili A, Bardini P, Aragno M, Parola M et al (2003) H_2O_2 and 4-hydroxynonenal mediate amyloid β-induced neuronal apoptosis by activation JNKs and p38 MAPK. Exp Neurol 180:144–155. doi:10.1016/S0014-4886(02)00059-6
37. Sinha Hikim AP, Lue Y, Yamamoto CM, Vera Y, Rodriguez S, Yen PH et al (2003) Key apoptotic pathways for heat-induced programmed cell death in the testis. Endocrinology 144(7):3167–3175. doi:10.1210/en.2003-0175
38. Nolan Y, Verker E, Lynch AM, Lynch MA (2003) Evidence that lipopolysaccharide-induced cell death is mediated by accumulation of reactive oxygen species and activation of p38 in rat cortex and hippocampus. Exp Neurol 184:794–804. doi:10.1016/S0014-4886(03)00301-7
39. Paasch U, Grunewald S, Fitzl G, Glander H (2003) Deterioration of plasma membrane is associated with activated caspases in human spermatozoa. J Androl 24:246–252
40. Song JJ, Lee YJ (2004) Daxx deletion mutant (amino acids 501–625)-induced apoptosis occurs through the JNK/p38-Bax-dependent mitochondrial pathway. J Cell Biochem 92:1257–1270. doi:10.1002/jcb.20155
41. Bhattacharyya A, Pathak S, Basak C, Law S, Kundu M, Basu J (2003) Execution of macrophage apoptosis by *Mycobacterium avium* through apoptosis signal-regulating kinase 1/p38 mitogen-activated protein kinase signaling and caspase 8. J Biol Chem 278:26517–26525. doi:10.1074/jbc.M300852200
42. Denial NN, Korsmeyer SJ (2004) Cell death: critical control points. Cell 116:205–219. doi:10.1016/S0092-8674(04)00046-7
43. Lee VY, McClintock DS, Santore MT, Budinger GR, Chandel NS (2002) Hypoxia sensitizes cells to nitric oxide-induced apoptosis. J Biol Chem 277:16067–16074. doi:10.1074/jbc.M111177200
44. Levine B, Huang Q, Isaacs JT, Reed JC, Griffin DE, Hardwick JM (1993) Conversion of lytic to persistent alphavirus infection by the bcl-2 cellular oncogene. Nature 361:739–742. doi:10.1038/361739a0
45. Grimm C, Wenzel A, Hafezi F, Reme' CE (2000) Gene expression in the mouse retina: the effect of damaging light. Mol Vis 6:252–260
46. Yamada K, Takane-Gyotoku N, Yuan X, Ichikawa F, Inada C, Nonaka K (1996) Mouse islet cell lysis mediated by interleukin-1-induced Fas. Diabetologia 39:1306–1312. doi:10.1007/s001250050574
47. Zender L, Hutker S, Liedtke C, Tillmann HL, Zender S, Mundt B et al (2003) Caspase 8 small interfering RNA prevents acute liver failure in mice. Proc Natl Acad Sci PNAS 100:7797–7802. doi:10.1073/pnas.1330920100